GENES, CHROMOSOMES & CANCER 55:864–876 (2016)

Analysis of Alternative Lengthening of Telomere Markers in *BRCA1* Defective Cells

Parisa K. Kargaran, Hemad Yasaei,[†] Sara Anjomani-Virmouni,[‡] Giovanna Mangiapane, and Predrag Slijepcevic*

Division of Biosciences, Department of Life Sciences, College of Health and Life Sciences, Brunel University London, Uxbridge, UK

Telomeres are specialized structures responsible for the chromosome end protection. Previous studies have revealed that defective *BRCA1* may lead to elevated telomere fusions and accelerated telomere shortening. In addition, BRCA1 associates with promyelocytic leukemia (PML) bodies in alternative lengthening of telomeres (ALTs) positive cells. We report here elevated recombination rates at telomeres in cells from human *BRCA1* mutation carriers and in mouse embryonic stem cells lacking both copies of functional *Brca1*. An increased recombination rate at telomeres is one of the signs of ALT. To investigate this possibility further we employed the C-circle assay that identifies ALT unequivocally. Our results revealed elevated levels of ALT activity in *Brca1* defective mouse cells. Similar results were obtained when the same cells were assayed for the presence of another ALT marker, namely the frequency of PML bodies. These results suggest that BRCA1 may act as a repressor of ALT.

INTRODUCTION

Telomeres are unique DNA–protein structures responsible for chromosome end protection. The loss of telomere function causes end-to-end chromosome fusion, cell cycle arrest and apoptosis or cellular senescence (Blasco et al., 1997; de Lange, 2015). In humans, telomere dysfunction leads to genetic and common diseases including cancer (Harley et al., 1990; Blackburn et al., 2015). Understanding the mechanisms behind telomere structural and length maintenance can be beneficial to understanding mechanisms of some human diseases, and also physiological processes such as aging.

Two tumor suppressors, BRCA1 and BRCA2, play a role in maintaining telomere integrity (McPherson et al., 2006; Min et al., 2012; Roy et al., 2012). BRCA1 is involved in DNA damage repair through nonhomologous end joining (NHEJ) and homologous recombination (HR) (Moynahan et al., 1999; Cao et al., 2003; Davalos and Campisi, 2003; Ohta et al., 2011). The lack of functional BRCA1 leads to radiosensitivity and telomere dysfunction (Foray et al., 1999; Trenz et al., 2002; Acharya et al., 2014; Sedic et al., 2015). The DNA damage sensor, the MRN complex, usually recruits BRCA1 to the DNA damage sites (Rosen, 2013). This acts as a signal for recruiting other proteins involved in the DNA double-strand break (DSB) repair pathways such as RAD51 (Rosen, 2013). It has also been shown that BRCA1 may have a role, through interacting with BLM and Rad50, in the alternative lengthening of telomere (ALT) pathway. However, the exact mechanism behind the potential BRCA1 role in ALT remains unclear.

Many DNA damage response proteins act as partners of BRCA1 in various pathways. In a recent study, it was shown that primary human mammary epithelial cells (HMECs) with mutations in *BRCA1* ($^{mut/+}$) show premature senescence as a result of genomic instability (Sedic et al., 2015). This unique type of cellular senescence caused by haploinsufficiency of a tumor suppressor is termed haploinsufficiency-induced senescence (HIS) (Sedic et al., 2015). The spontaneous bypass of this senescence pathway is thought to be involved in the early onset of breast cancer in individuals with *BRCA1* mutations

Additional Supporting Information may be found in the online version of this article.

[†]Present address: School of Cellular and Molecular Medicine, Biomedical Sciences Building, University of Bristol, University Walk, Clifton, Bristol, UK

[‡]Present address: The Institute of Cancer Research, Chester Beatty Laboratories, London, UK

*Correspondence to: P. Slijepcevic; Division of Biosciences, Department of Life Sciences, College of Health and Life Sciences, Brunel University London, UB83PH, UK.
E-mail: predrag.slijepcevic@brunel.ac.uk

Received 14 February 2016; Revised 3 June 2016; Accepted 3 June 2016

DOI 10.1002/gcc.22386

Published online 26 July 2016 in Wiley Online Library (wileyonlinelibrary.com).

(Sedic et al., 2015). Although these immortalized nontumorigenic *BRCA1* $^{mut/+}$ HMECs showed rapid genomic instability, increased DNA damage and telomere erosion, the exact mechanism by which the telomere maintenance is affected is not known (Sedic et al., 2015). Recent findings suggest that BRCA1 accumulates at telomeres in the ALT-positive cancer cells, most likely with the help of BLM and PML bodies (Acharya et al., 2014). Furthermore, BRCA1 may be involved in end-processing and fusion of uncapped telomeres through the A-NHEJ (alternative NHEJ) pathway together with its interacting partner CtIP (Badie et al., 2015).

The activities of BRCA1 and BLM at telomeres have only been recognized recently (Acharya et al., 2014). BRCA1 is required for recombination proteins to promote strand processing and invasion and to form recombination intermediates. The process requires BLM during G2 phase of the cell cycle (Acharya et al., 2014). However, this role is different from the role played by the BRCA1–RAD50 complex during the Sphase (Maser and DePinho, 2002; Davalos and Campisi, 2003). Although BRCA1 may have an important functional role in the ALT pathway (which utilize HR for telomere length homeostasis), the mechanism of this process is not fully understood.

This study provides further evidence for the involvement of BRCA1 in telomere maintenance and shows that the lack of functional BRCA1 may enhance levels of the ALT activity.

MATERIALS AND METHODS

Cell Lines and Culture Conditions

Lymphoblastoid cell lines from *BRCA1* mutation carriers (GM14090 and GM13705) and a control cell line (GM00893) were obtained from the Coriell Cell Repository and maintained in RPMI1640 medium (Gibco, Thermo Fisher Scientific, Waltham, MA) supplemented with 10% fetal calf serum as described previously (Castilla et al., 1994; Struewing et al., 1995). The HCC1937 cell line was kindly provided by Dr M. Zdzienicka, University of Leiden the Netherlands and maintained in RPMI 1640 medium (Gibco, Thermo Fisher Scientific, MA) with 15% fetal calf serum. Mouse embryonic stem cells (mESCs) E14 and E408 (from here on referred to as 408) were kindly provided by Dr Beverly Koller Duke University (United States) and were cultured at 37°C in the atmosphere of 5% CO_2 on Gelatine (Sigma-Aldrich, St Louis, MO) coated dishes in Knockout Dulbecco's modified Eagle's minimal essential medium (D-MEM) (Gibco, Thermo Fisher Scientific, MA) and supplemented with 20% KnockOut serum replacement as described (Snouwaert et al., 1999). U2OS and G292 cell lines were cultured in the McCoys 5A medium (Gibco, Thermo Fisher Scientific, MA), supplemented with 10% fetal bovine serum. HeLa and SKLU-1 cell lines were cultured in the D-MEM supplemented with 10% fetal bovine serum. All cell lines were maintained at 37°C (humidified incubator LEEC) with 5% carbon dioxide content except HeLa and U2OS, which were maintained in the atmosphere containing 10% of carbon dioxide. Details of all cell lines used in this study including the type of *BRCA1* mutation is listed in Supporting Information Table S1.

Irradiation

Cells were exposed to ionizing radiation using a $Cobalt^{60}$ source (0.6859 Gy min^{-1}). Adherent cells were grown to 80–90% confluence either in nonfiltered tissue culture flasks (Nunc, Thermo Fisher Scientific, MA) for metaphase preparation, or on Poly-prep slides (Sigma-Aldrich) depending on the experimental protocol. Cells were exposed to different doses of ionizing radiation including: 0.5 Gy, 1.0 Gy, 2.0 Gy, and 4.0 Gy.

Telomere Sister Chromatid Exchange (T-SCE) Analysis Using Chromosome Orientation Fluorescence *In Situ* Hybridization (CO-FISH)

Metaphase preparation and CO-FISH were performed as described (Bailey et al., 2004). Cells were split and subcultured in the fresh medium containing a 3:1 ratio of 5-bromo-2-deoxyuridine:5-bromodeoxycytidine (Sigma-Aldrich) at a final concentration of 1×10^{-5} M for 24 hr for human and 17 hr for mouse cell lines. Colcemid (0.1 μg/ml) was added for the final 4 hr of incubation.

Immunofluorescence

The list of all antibodies is shown in Supporting Information Table S2. In brief, cells were washed with phosphate buffered saline (PBS) and then permeabilized for 10 min on ice with cold PBS and 0.5% triton X-100 (Sigma-Aldrich). The cells were washed with cold PBS 4 × 5 min and were blocked with 0.2% (w/v) cold water fish gelatin (Sigma G-7765), 0.5% (w/v) BSA (Sigma A-2153) in PBS for at least 30 min at room temperature. Primary antibodies were diluted according to Supporting Information Table S2 and incubated for 1

hr at room temperature. The secondary antibodies were added again according to the dilutions set out in Supporting Information Table S1 for 1 hr following three rounds of washes in PBS with 1% tween-20. The slides were washed in PBS and Cy3-conjuated PNA probe $(CCCTAA)_3$ was applied for 2–3 min at 80°C, followed by standard formamide and saline-sodium citrate (SSC) washes. Finally, cells were mounted with coverslips using 4′, 6′-diamidino-2-phenylindole (DAPI)-containing mounting medium (Vector Laboratories, Burlingame, CA).

Telomere Dysfunction-Induced Foci (TIF) Analysis

Combined immunofluorescence (γ-H2AX) and FISH (telomeric PNA probe) to detectDNA damage at telomeres is usually known as TIFs (Yasaei and Slijepcevic, 2010). First, detection of γ-H2AX foci by immunofluorescence was performed. Slides were incubated overnight in a dark container at room temperature. The following day, FISH with a Cy3-conjugated PNA telomeric probe $(CCCTAA)_3$ as described above, was performed followed by formamide and SSC washes. Cells were counterstained with DAPI. The slides were analyzed using the computerized Zeiss Axioskop 2 fluorescence microscope equipped with a CCD camera and Metasystem software (Altlussheim, Germany).

Telomere Length Analysis Using Interphase Quantitative FISH (IQ-FISH)

To measure telomere signals in the interphase nuclei we followed a protocol previously described (Ojani, 2012). A total of 50 interphase cells per cell line were analyzed and the mean telomere fluorescence intensity was determined for each cell line. The integral part of the method is the use of two mouse lymphoma cell lines, LY-R and LY-S, as calibration standards. These cell lines have stable telomere lengths of 49 kb and 7 kb, respectively (McIlrath et al., 2001; Cabuy et al., 2004, 2005; Yasaei and Slijepcevic, 2010). Using the values of telomere fluorescence obtained for LY-R and LY-S cells, the corrected calibrated fluorescence (CCFL) was calculated for the two human lymphoblastoid cell lines BRCA1 defective cell lines (GM13705 and GM14090) and mESCs (E14 and 408) using the following formula: $CCFL = CF \times FL_{x,}$ where CF is the final correction factor, CCFL represents Corrected Calibrated Fluorescence and FL_x represents unmodified fluorescence of the sample under investigation.

Telomerase Repeat Amplification Protocol (TRAP)

We followed the manufacturer's guidelines for the TRAP assay (Millipore, Billerica, MA) and these have been described in detail previously (Kim et al., 1994; Yang et al., 2007). All cell pellets were resuspended in the 3-[(3-cholamidopropyl)-dimethylammonio]-1-propanesulfonate (CHAPS; Millipore Company) detergent lysis method. The protein concentration of the samples was determined using the Pierce BCA Protein Assay Kit (Thermo Scientific) according to the manufacturer's protocol. For all TRAP PCRs, we used 200 ng of CHAPs lysed protein and performed three-independent experiments.

C-Circle Assay

The full working protocol of C-circle (CC) assay was kindly provided by Prof Roger Reddel (Children's Medical Research Institute, University of Sydney, Australia) and described in detail previously (Henson et al., 2009). In short, the level of CC is measured through a two-step process: DNA amplification using Phi-29 DNA polymerase and nucleotide lacking dCTP followed by radiolabeled (P^{32}) probing and hybridization using $(CCCTAA)_3$ oligonucleotide. Total genomic DNA was extracted from cell pellets of various cell lines using QIAmp DNA Mini Kit (Qiagen, Hilden, Germany) by following the manufactures guideline. 20 ng or 30 ng gDNA was used for all PCRs according to the published protocols (Henson et al., 2009).

Immunoblotting

Western blot analysis was performed to quantify the BRCA1 protein expression. A total of 15×10^5 cells were centrifuged and washed with ice-cold PBS and lysed in lysis buffer (Tris-HCl (1 M, pH 7.4), NaCl (5 M), EDTA (0.5 M, pH 8.0), Triton X-100 (1%), SDS (10% w/v), Na-deoxycholate (10% w/v), Protease Inhibitor (Roche Diagnostics, Penzberg, Germany) (7×) nuclease-free water and incubated on ice. The protein extracts were mixed with SDS-PAGE loading buffer and loaded in a gradient gel (Mini-Protean TGX stain-free gels, Bio-rad, Hercules, CA), were transferred to a PVDF membrane (Thermo Fisher Scientific). The primary antibodies were used were BRCA1 and β-Actin as a loading control. The HRP-conjugated, secondary antibodies used were anti-mouse IgG and anti-goat.

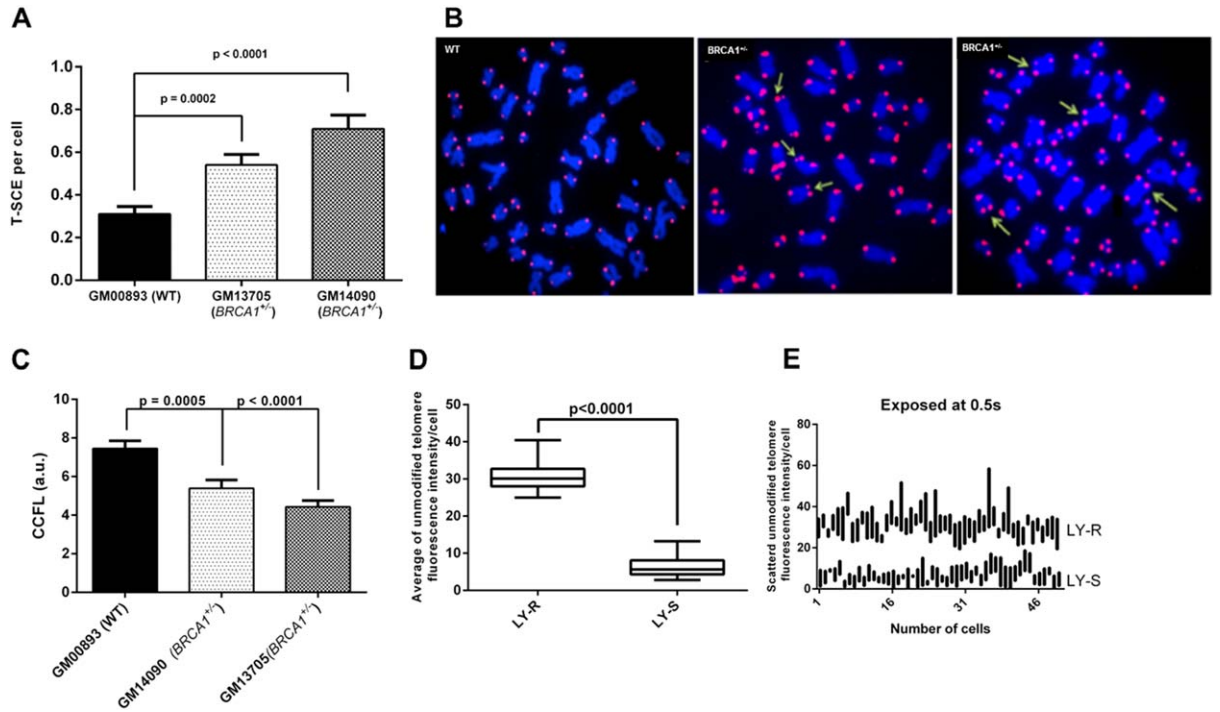

Figure 1. Human *BRCA1* heterozygote lymphoblastoid cells show higher levels of sister chromatid exchanges: (A) CO-FISH analysis for telomere sister chromatid exchanges revealed a significantly higher level of T-SCE in the two *BRCA1* heterozygote cells compared with the normal counterpart. (B) Examples of CO-FISH showing elevated levels of T-SCE (arrows). (C) Telomere length measurement using interphase Q-FISH showed significantly shorter telomeres in the two *BRCA1* heterozygote cells. (D) The average telomere lengths of the LY-R and LY-S mouse lymphoblastoid cells were used to normalize the telomere probe intensity. (E) An average of 50 interphase nuclei was measured from the two mouse cells. All exposures were fixed at 0.5 sec. Error bars represent standard error of the mean (SEM). In all cases a minimum of 50 cells was analyzed in two-independent experiments. Note: HCC1937 ($BRCA1^{+/-}$) cell line had CCFL of 6.95 (SEM 0.84) when normalized to the LY-R and LY-S cells. 50 HCC1937 cell nuclei were scored for IQ-FISH measurement. [Color figure can be viewed in the online issue, which is available at wileyonlinelibrary.com.]

Statistical Analysis

All statistical tests and graphical drawings were performed on GraphPad PRISM version 6. Student *t*-test was used for all statistical analyses with 95% confidence interval ($\alpha = 0.05$) unless otherwise stated.

RESULTS

Human *BRCA1* Mutation Carrier Cells Show Elevated T-SCE Frequencies

We have previously demonstrated that lymphoblastoid cell lines from *BRCA1* mutation carriers (GM14090 and GM13705) show signs of telomere dysfunction as evidenced by the increase in chromosome end-to-end fusion (Al-Wahiby and Slijepcevic, 2005). This was accompanied by telomere shortening as measured by the conventional Q-FISH. To investigate if there are other signs of telomere dysfunction in these lines we analyzed spontaneous frequencies of T-SCEs using the CO-FISH technique. We found, on average, a twofold higher frequency of T-SCEs in the *BRCA1* mutation carrier cell lines relative to the control cell line (Figs. 1A and 1B). In a total of 200 cells analyzed we observed 142 and 108 T-SCEs in GM14090 and GM13705, respectively, compared with only 62 T-SCEs in the control cell line (Figs. 1A and 1B). To confirm that *BRCA1* mutation carrier cell lines show shorter telomeres we performed IQ-FISH. This technique relies on the higher number of cells than the conventional Q-FISH, thus increasing the statistical power. In line with our previous observation (Cabuy et al., 2005), the IQ-FISH data showed that *BRCA1* mutation carrier lines had significantly shorter telomeres compared with the control line ($P < 0.0001$) (Figs. 1C–1E).

Next, we analyzed the frequencies of TIFs in the above-mentioned cell lines. The cell lines from *BRCA1* mutation carriers showed a twofold increase in the levels of spontaneous γ-H2AX foci relative to the control cell line (Fig. 2A and Supporting Information Fig. S1A) suggesting higher levels of unrepaired DNA DSBs due to lack of

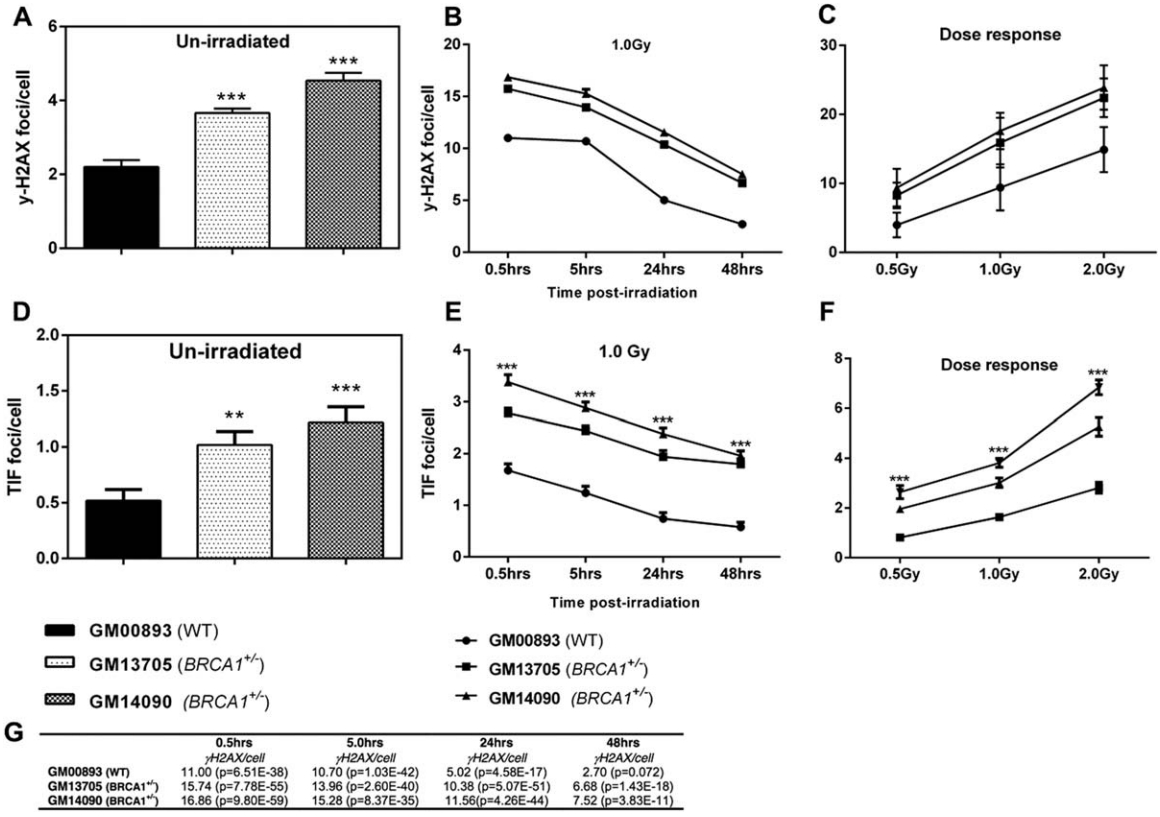

G

	0.5hrs γH2AX/cell	5.0hrs γH2AX/cell	24hrs γH2AX/cell	48hrs γH2AX/cell
GM00893 (WT)	11.00 (p=6.51E-38)	10.70 (p=1.03E-42)	5.02 (p=4.58E-17)	2.70 (p=0.072)
GM13705 (BRCA1+/-)	15.74 (p=7.78E-55)	13.96 (p=2.60E-40)	10.38 (p=5.07E-51)	6.68 (p=1.43E-18)
GM14090 (BRCA1+/-)	16.86 (p=9.80E-59)	15.28 (p=8.37E-35)	11.56(p=4.26E-44)	7.52 (p=3.83E-11)

Figure 2. Analysis of the kinetics of repair of γ-H2AX and TIF revealed telomere dysfunction phenotypes: (A) Levels of spontaneously induced γ-H2AX. (B) Repair kinetics after 1.0 Gy of radiation-induced γ-H2AX showing delayed repair kinetics in the two human BRCA1 heterozygote lymphoblastoid cells. (C) A dose–response curve showing γ-H2AX levels after 0.5 Gy, 1.0 Gy, and 2.0 Gy of the IR. (D) Spontaneous levels of TIFs in the two *BRCA1* heterozygous lymphoblastoid cells. (E) A significantly higher levels of TIFs persist 48 hr after 1.0 Gy IR in the two *BRCA1* heterozygous lymphoblastoid cells. (F) Similar differences in the levels of TIFs in the two lymphoblastoids *BRCA1* heterozygous cells when exposed to 0.5 Gy, 1.0 Gy, and 2.0 Gy of IR with levels of TIFs peaking at 2.0 Gy. (G) *t*-Test analysis comparing untreated γ-H2AX foci per cell in each sample with 1.0 Gy irradiation. Asterisks indicate the level of significance ($^{**}P < 0.01$, $^{***}P < 0.001$). Error bars represent SEM. In all experiments a minimum of 50 cell nuclei was analyzed in at least two-independent experiments.

functional BRCA1. As expected, the repair of DNA DSBs in *BRCA1* mutation carrier lines was significantly delayed relative to the control line (Fig. 2B). Furthermore, DNA damage followed a dose–response pattern with a clear distinction between the normal line and *BRCA1* mutation carrier lines (Fig. 2C).

When the spontaneous levels of TIF were analyzed, we found 1.0–1.2 TIFs/cell in *BRCA1* mutation carrier cells compared with 0.5 TIFs/cell in the control line (Fig. 2D and Supporting Information Fig. S1A). The kinetics of TIFs after exposure of the cells to IR revealed inability of *BRCA1* mutation carrier lines to restore the TIFs frequency to preirradiation levels unlike the control line (Fig. 2E). The dose-response analysis revealed dramatic increase in TIF frequency in *BRCA1* mutation carrier lines (Fig. 2F).

Taken together these results suggest that BRCA1 is implicated in telomere maintenance. Importantly, the significant increase in T-SCEs frequencies in *BRCA1* mutation carrier lines could be indicative of ALT activity as T-SCEs are usually elevated in ALT-positive cell lines (Londono-Vallejo et al., 2004; Neumann and Reddel, 2006).

Elevated T-SCEs in *Brca1* Defective Mouse Cells

To investigate if increased frequencies of T-SCEs occur regularly as a result of BRCA1 dysfunction we used the $Brca1^{-/-}$ mESC line, 408, and its normal counterpart, E14 (Snouwaert et al., 1999). We found a nearly threefold higher T-SCE frequency in the 408 cell line relative to the control E14 cell line (Figs. 3A and 3B). In addition, we observed a twofold increase in telomere fusions in 408 cells (Figs. 3C and 3D) and significantly shorter telomeres relative to the control line (Figs. 3E and 3F). The analysis of DNA damage foci (Figs. 4A and 4B) and TIFs (Figs. 4C and 4D) revealed, similarly to human lines, inability of 408 cells to repair DNA damage and TIFs to

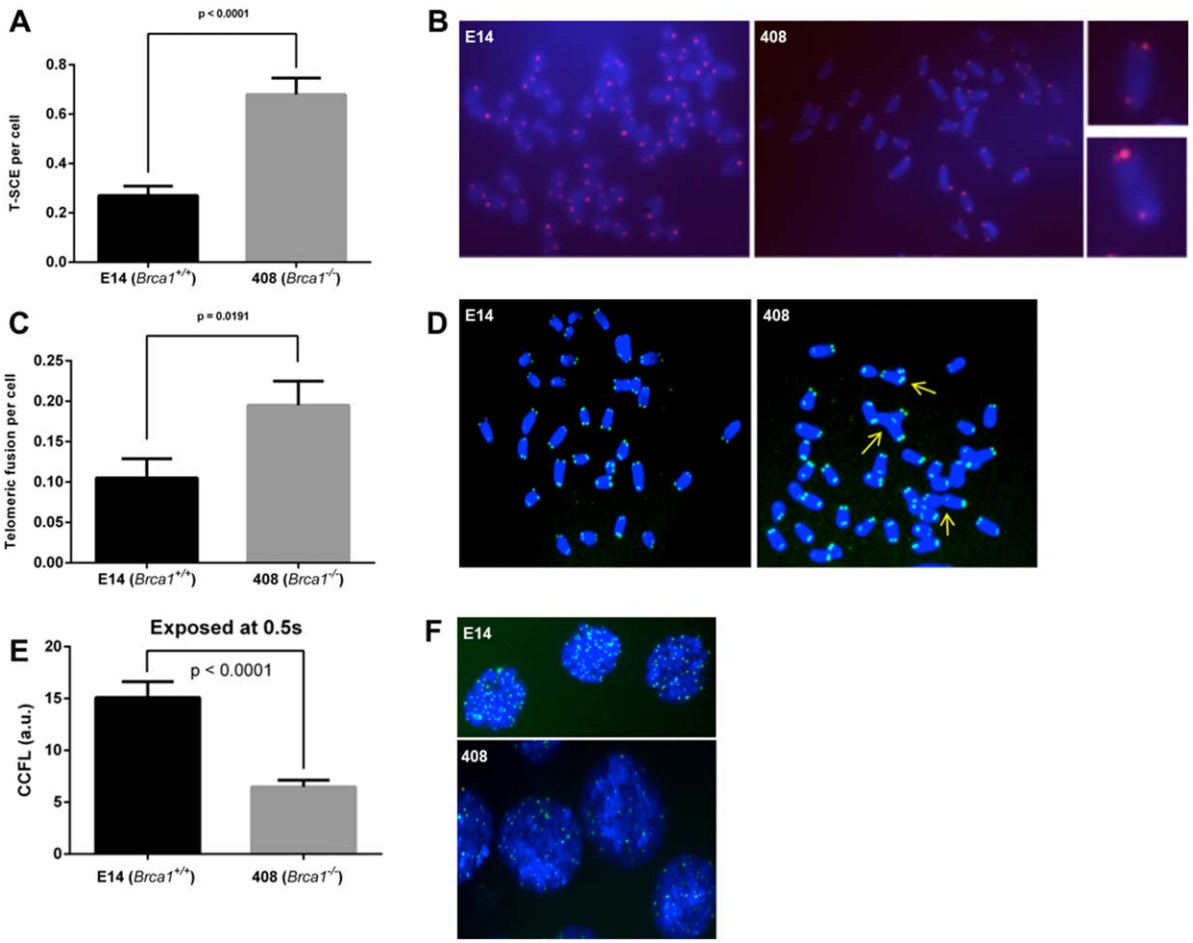

Figure 3. Sister chromatid exchanges, telomeric fusions and telomere length analysis reveals dysfunctional telomeres in the Brca1 defective mESCs: (A) CO-FISH analysis reveals increased levels of T-SCEs in the *Brca1* defective mESC (408). (B) CO-FISH example showing T-SCEs measured in the two mESCs. (C) Telo-FISH analysis showing higher levels of spontaneously generated telomeric fusions in the *Brca1* defective 408 cells. (D) Examples of telomeric fusions in the two mESCs. Arrow showing sites of telomeric fusions. (E) Telomere length analysis using interphase Q-FISH normalized to the LY-R and LY-S cells. The data show threefold reduction in the telomere lengths in the 408 *Brca1* defective mESC. (F) Examples of interphase cells with telomeric probes in green. A reduced telomeric signal is seen in the 408 cells. A total of 50 metaphases was analyzed in two-independent experiments. A minimum of 50 cell nuclei was captures and telomeric signal measured with exposure set at 0.5 sec in two-independent experiments. Error bars indicate SEM. [Color figure can be viewed in the online issue, which is available at wileyonlinelibrary.com.]

preirradiation levels in comparison with the control E14 line (Supporting Information Fig. S1B). The only difference was an extremely high spontaneous frequency of γ-H2AX foci in mESCs (Fig. 4A) in comparison with human lines (Fig. 2A). This is in agreement with previous reports that suggested that elevated frequencies of γ-H2AX in mESCs could result from epigenetic mechanisms rather than from DNA damage (Turinetto et al., 2012). In addition, the analysis of radiation-induced chromosomal aberrations revealed greater sensitivity of 408 cells (Figs. 4E and 4F). Therefore, these results suggest that *Brca1*$^{-/-}$ mESCs show clear telomere dysfunction and confirm that frequencies of T-SCEs are elevated relative to control cells.

C-Circle Analysis Reveals Increased ALT Activity in the Brca1 Defective Mouse Embryonic Stem Cells

Since we observed higher levels of T-SCEs in human and mouse cells lacking functional BRCA1 relative to control cells, and given that frequencies of T-SCEs are elevated in ALT-positive cell lines (Londono-Vallejo et al., 2004; Neumann and Reddel, 2006), this observation could be indicative of a potential ALT activity in affected cells. The gold standard method for identifying ALT activity is the CC assay (Henson et al., 2009; Henson and Reddel, 2010). Therefore, to investigate if the observed elevated T-SCE frequencies represent a sign of ALT activity we performed the CC assay in (i) cell lines with dysfunctional *BRCA1* and (ii)

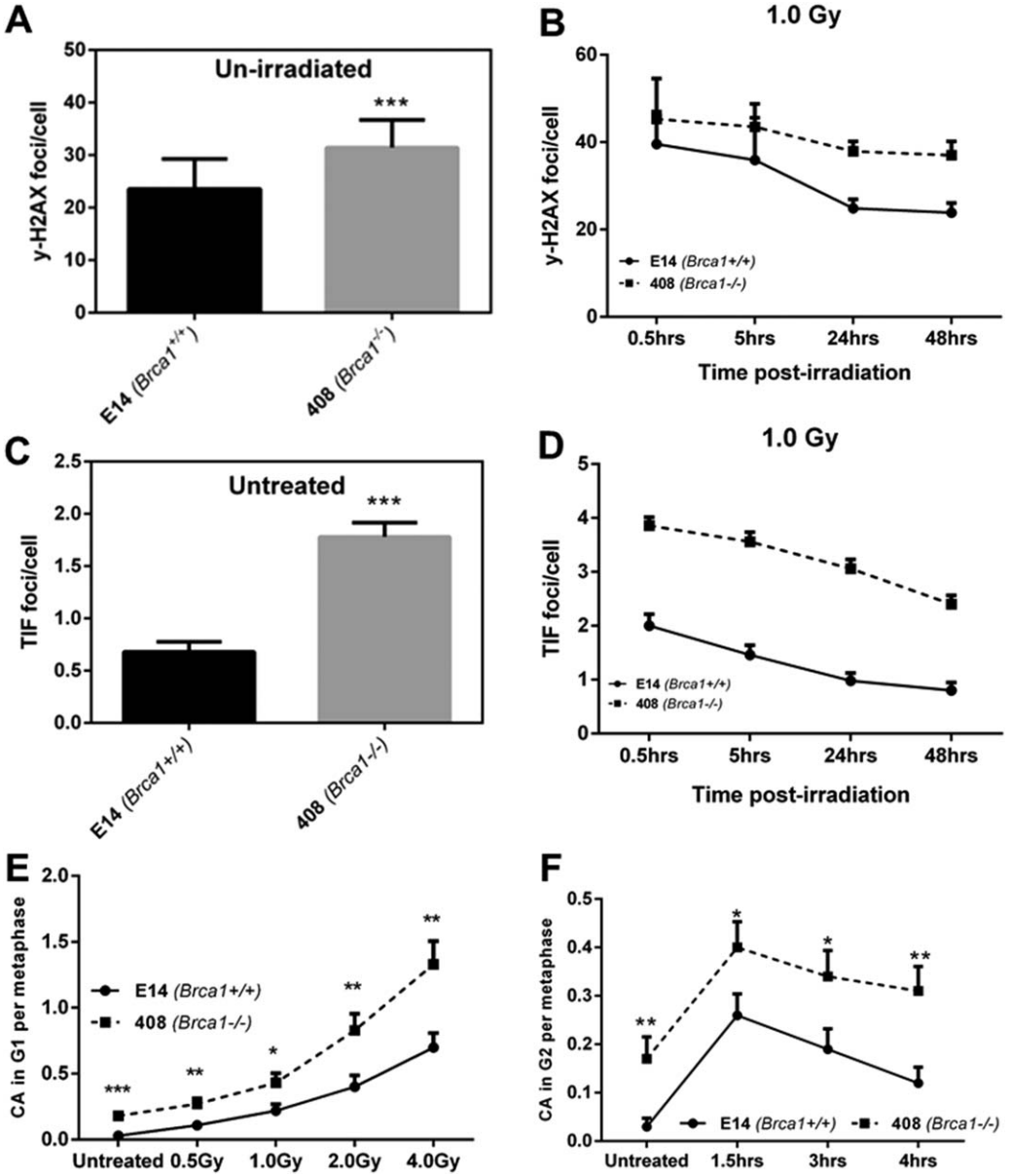

Figure 4. γ-H2AX, TIF and chromosomal aberration analysis in the *Brca1* defective mouse embryonic stem cells: (A) Spontaneous levels of γ-H2AX in the mouse *Brca1* wt (E14) and defective (408) ES cells. (B) Repair kinetics measured using γ-H2AX after exposure to 1.0 Gy of IR. (C) Levels of spontaneous TIFs in the two mESCs. (D) Mean TIF levels in the two mESCs showing a delayed repair of the telomeres. (E) A dose response curve of CA measured in the G1-phase after exposures to 0.5 Gy, 1.0 Gy, 2.0 Gy, and 4.0 Gy of the IR. (F) A time-course experiment showing frequencies of CA measured in the G2-phase after exposure to 1.0 Gy. A minimum of 50 cell nuclei was analyzed for γ-H2AX and TIFs and 100 metaphase cells analyzed for CA studies in two-independent experiments. Asterisks indicate the level of significance ($^{**}P < 0.01$, $^{***}P < 0.001$). Error bars represent SEM. CA, chromosomal aberration.

a range of control ALT- or telomerase-positive cell lines (Supporting Information Table S1).

As expected, ALT-positive cell lines (U2OS, SKL-U1, and G292) showed a robust ALT activity (Fig. 5A). To investigate ALT in other cell lines in a quantitative way we normalized the values observed so that the value observed for the U2OS cell line represents 1 arbitrary unit (a.u.) (Fig. 5A). We have also generated a calibration curve using serial dilutions of gDNA from the U2OS cell line (Fig. 5C). None of the human telomerase-positive cell lines, such as HeLa (Fig. 5E) and a cell line from a *BRCA1* mutation carrier (GM13705) or the cell line completely lacking functional *BRCA1* (HCC1937; see Fig. 5D; telomerase activity data not shown), exhibited visible ALT activity, at least after the quantification based on analyzing images with the J-image software when using

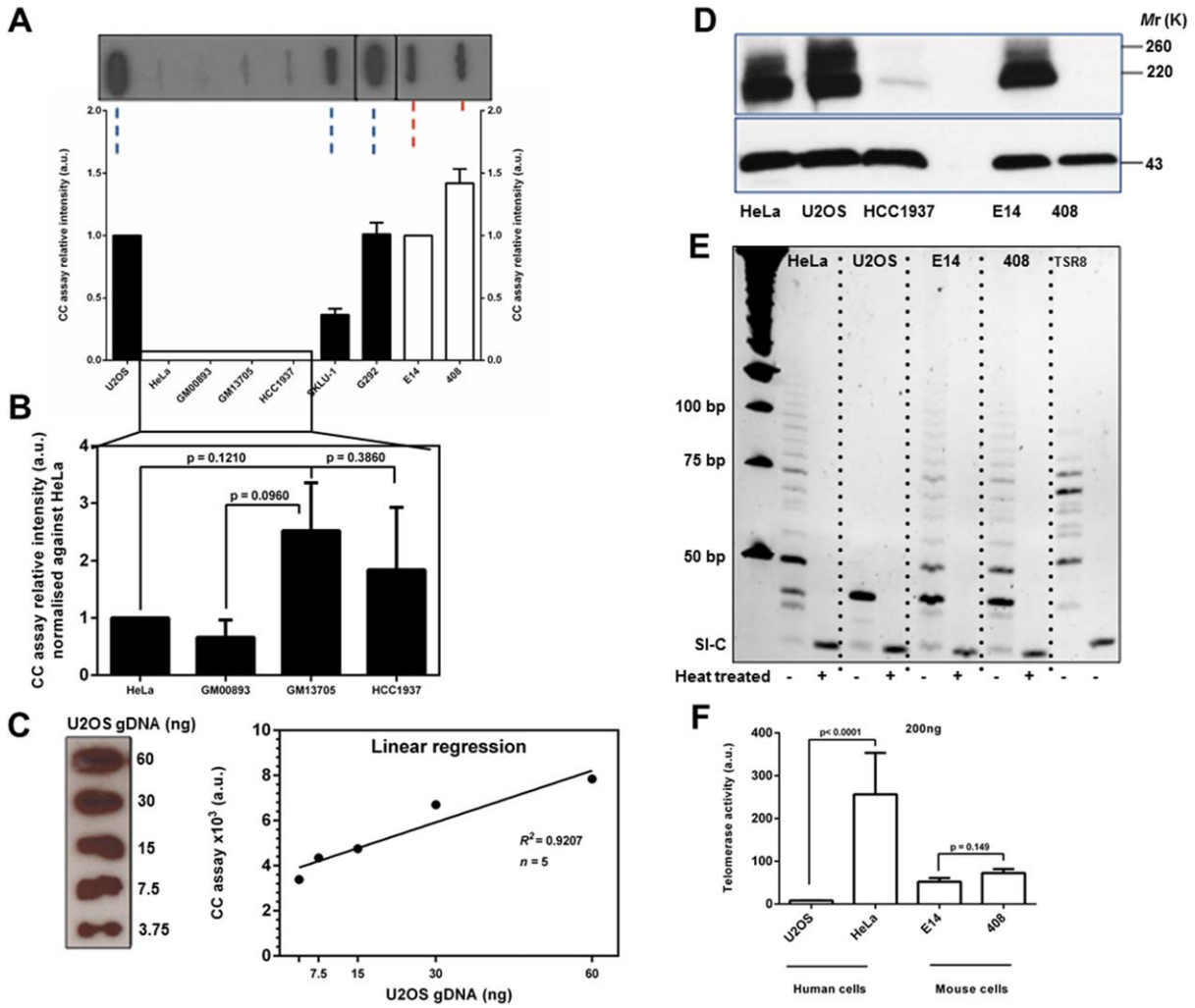

Figure 5. C-circle assay showed ALT activity in the mESCs: (A) CC assay indicating recombination activity normally associated with ALT. 20 ng of gDNA were used to measure levels of CC and quantified relative to the U2OS for the human cells and E14 for the mouse cells. The two mouse ESCs show ALT activity with the *Brca1* defective 408 showing higher ALT activity. (B) Four human telomerase-positive cell lines () showed basal ALT activity and when measured using the Image J analysis software, elevated ALT activity in the two *BRCA1* defective cell lines (GM13705 and HCC1937) compared with the control counterparts. (C) U2OS ALT-positive human cells used to draw a standard curve and showing the sensitivity of the assay. (D) Immunoblotting showing lack of Brca1 in the mouse 408 cells and reduced BRCA1 activity in the human breast cancer cells HCC1937. Anti-beta actin used as loading control. (E) TRAP assay revealing telomerase activity in 200 ng of CHAPS-lysed protein lysate of the human HeLa and HCC1937 cancer cells but not in the U2OS osteosarcoma cells. Both mouse ESCs show telomerase activity but the activity is lower in the 408 cells. (F) Quantification of the TRAP gel measuring the telomerase activity from 200 ng of the CHAPS-lysed protein lysate. Three TRAP assays were performed using three-independently extracted lysates. TSR8 is the quantitation control. SI-C is the standard internal control. Heat treatment was done at 95°C for 10 min. The error bars indicate standard deviation. [Color figure can be viewed in the online issue, which is available at wileyonlinelibrary.com.]

U2OS as the normalizing standard (Fig. 5A). However, some signals are visible in the lanes representing the HeLa, GM00893, GM13705, and HCC1937 cell lines suggesting that the value of CC activity is not 0 in these lines. When the signal generated for the U2OS line is used as the normalizing standard it leads to 0 values in cells with weak signals.

To investigate whether weak signals differ between themselves we used the signal generated by the HeLa cell line as the normalizing standard. This analysis, revealed that the GM13705 and HCC1937 cell lines show higher ALT activity than the HeLa and GM00893 cell lines (Fig. 5B), however, the increase was not significant ($P = 0.1210$). All four human cell lines featuring weak CC-assay signals showed telomerase activity (Fig. 5E and data not shown).

In contrast to human telomerase-positive cell lines in which ALT activity was detectable but

very low, both mouse cell lines showed a strong ALT activity (Fig. 5A). The control E14 cell line had a degree of ALT activity comparable to that in the U2OS cell line, whereas the *Brca1*$^{-/-}$ 408 cell line showed the highest recorded ALT activity: ~50% higher than that measured in the U2OS and E14 cell lines ($P = 0.0341$) using 30 ng of gDNA (Fig. 5A). We observed a similar significant difference in the CC-activity when using 20 ng of gDNA between E14 and 408 cells (data not shown) ($P = 0.0119$). Mouse cell lines did not differ in terms of telomerase activity (Figs. 5E and 5F). These results are in line with a recent study that showed coexistence of the ALT activity and telomerase in mouse cells (Perrem et al., 2001; Neumann et al., 2013). Our results suggest that the ALT activity is significantly elevated in the mouse Brca1 defective environment.

Immunofluorescence Analysis

In addition to the CC assay another indicator of ALT is detection of APBs (ALT-associated PML Bodies) (Yeager et al., 1999; Henson et al., 2002; Neumann and Reddel, 2006). We observed a significant difference between the 408 and E14 cell lines in the levels of APBs ($P = 0.0002$) (Fig. 6A). This also held true for the HCC1937 cell line that lacks functional *BRCA1* when compared with the HeLa cell line (Fig. 6A) as well as two BRCA1 defective lymphoblastoid cell lines (GM13705 and GM14090, $P = 0.0294$ and $P = 0.004$, respectively) when compared with the BRCA1 wt GM00893 (Supporting Information Fig. S2A). However, when we analyzed the colocalization of APBs with telomeres, we did not observe any significant difference between 408 and E14 cells, HCC1937 and HeLa cells, or GM13705/GM14090 and GM00893 (Fig. 6B and Supporting Information Figs. S2A–2C).

It has been shown recently that BLM colocalizes with BRCA1 within telomeres in ALT-positive human cells (Acharya et al., 2014). The BLM RecQ helicase functions at telomeres to regulate the D-loop formation following strand invasion and may also be involved in resolving recombination events in mortal and telomerase-positive cells as well as in ALT-positive human cells (Cheng et al., 2006; Acharya et al., 2014). We did not find any difference in the levels of BLM-positive foci between the E14 and 408 cells (Fig. 6C), whereas the levels of BRCA1 foci including its colocalization with telomeres were found to be significantly lower in the BRCA1 defective human and mouse cells as expected (Supporting Information Figs. S3C and 3D). By contrast, we observed a significant difference in the frequencies of BLM-positive foci between the HCC1937 cell line and the HeLa and U2OS cell lines (Fig. 6C). However, when we analyzed colocalization of BLM with telomeres we found that the 408 and HCC1937 cell lines had significantly fewer colocalizations with telomeres than the *BRCA1* wt cells lines (E14 and U2OS) (Fig. 6D and Supporting Information Fig. S2D). This could be due to the fact that BRCA1 is required for BLM colocalization at telomeres (Fig. 6F and Supporting Information Figs. S2E and S4B) as suggested previously (Acharya et al., 2014).

A recent study indicated that mutations in ATRX (alpha thalassemia/mental retardation syndrome X-linked) are associated with ALT activation in 90% of human ALT-positive cells (Lovejoy et al., 2012). As expected, the U2OS cell line did not show staining with the ATRX antibody in contrast to nonALT cell lines (Supporting Information Fig. S3A). No differences were observed in the frequencies of ATRX-positive foci between the 408 and E14 cell lines, or the HeLa and HCC1937 cell lines (Supporting Information Fig. S3A). Furthermore, no differences were observed in colocalization between ATRX-positive foci and telomeres between the 408 and E14 cell lines or the HeLa and HCC1937 cell lines (Supporting Information Figs. 3A and 3B). When we looked for colocalization of ATRX with telomeres, we did not find any significant differences between in ATRX colocalization with telomeres in the mESC E14 and 408 cell lines (Supporting Information Figs. S3A and 3B), whereas the two mESC lines showed high frequencies of ATRX in contrast to published work where ATRX was mutated in the ALT-positive human cells, including U2OS (Lovejoy et al., 2012). Finally, when we looked at colocalization of BRCA1 with ATRX and BLM (Figs. 6E and 6F, Supporting Information Figs. S2E and S4), a high ATRX colocalization in the telomerase-positive cells (HCC1937 and HeLa), was observed, which is in-line with previous observation, highlighting the fact that ALT marker activity seen in the human BRCA1 defective sample, such as T-SCE, APBs, shorter and heterogeneous telomeres, may be due to ALT activity in these cells but may not directly be involved in maintaining telomere length as this is carried out by the telomerase enzyme (Supporting Information Fig. S3E). However, further experiments are needed to prove this hypothesis.

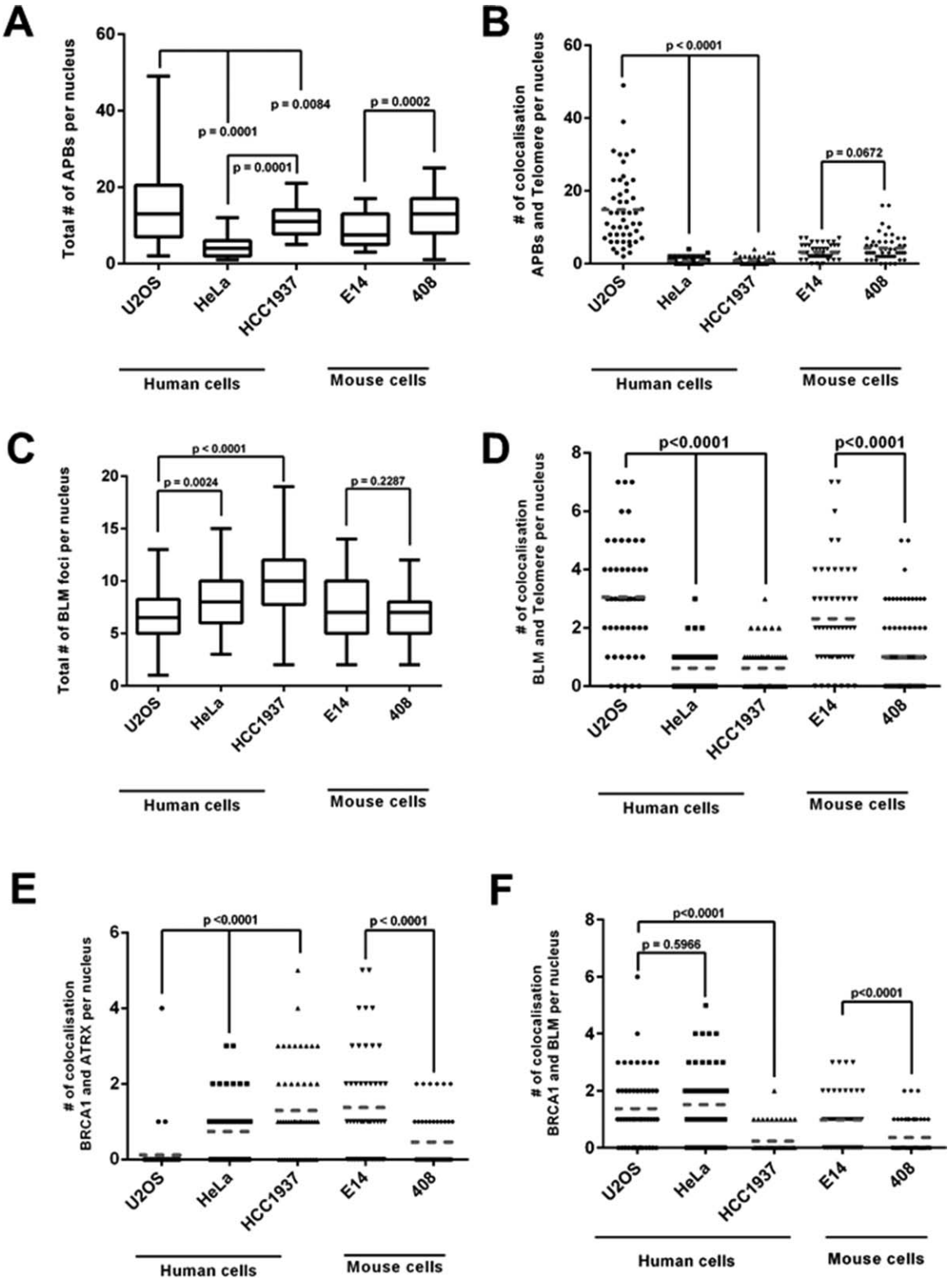

Figure 6. Double immunofluorescence analysis of APBs, BRCA1, ATRX, BLM in the human and mouse cells: (A and B) Total number of ALT-associated PML bodies (APBs) in the human and mouse cells. There were significantly higher levels of APBs in the U2OS ALT-positive human cells and the Brca1 defective mESC 408; however, the levels of APBs associated with telomeres were not significantly different in the mESC 408 but was much higher in the U2OS cells. (C and D) Reduced BLM foci were observed in the U2OS ALT-positive human cells but not in the ALT negative human or the ALT-positive mouse cells. However, BLM colocalizations with telomeres were significantly higher in the U2OS and Brca1 wt mESC E14. (E) Colocalization of BRCA1 with ATRX, and (F) BRCA1 with BLM, reveal differences between human and mouse cells. A minimum of 50 cell nuclei was analyzed in two-independent experiments in all the samples shown above. The error bars represent min/max in the whisker box plot and the gray dotted line indicates mean in the scatter graphs. *t*-Test used for statistical analysis with alpha set at 0.05.

DISCUSSION

Previous studies have shown that defects in *BRCA1* cause telomere alterations including increased frequencies of telomeric fusion and telomere shortening (Al-Wahiby and Slijepcevic, 2005; Cabuy et al., 2005, 2008; French et al., 2006; McPherson et al., 2006) thus suggesting an active role of BRCA1 in telomere maintenance. Here, we provide further evidence for the BRCA1 involvement in telomere damage maintenance generated spontaneously or after exposure to ionizing radiation (Figs. 2D–2F, 4B and 4D, and Supporting Information Fig. S5). Furthermore, there is evidence that BRCA1 colocalizes with APBs in ALT-positive cells (Acharya et al., 2014). The results presented in this paper also support earlier findings and provide further evidence for the role of *BRCA1* in telomere homeostasis. Similarly to cells lacking BLM and WRN, proteins affected in Bloom and Werner syndrome patients (Salk et al., 1985; Laud et al., 2005), we have shown that *BRCA1* defective cells harbor high frequencies of T-SCEs (Figs. 1A and 3A). However, we did not observe any increases in the T-SCEs levels in the HCC1937 cell line (data not shown) similar to previously published data (Al-Wahiby and Slijepcevic, 2005). In contrast, the levels of T-SCEs in the ALT-positive U2OS cells were much higher than in the ALT-negative HeLa cells as shown previously (Anjomani Virmouni et al., 2015). Interestingly, the frequencies of T-SCEs are also elevated in *BRCA2* defective cells (Sapir et al., 2011; Bodvarsdottir et al., 2012). Given that T-SCEs are one of the hallmarks of ALT this prompted us to employ the CC assay, a method that detects ALT unequivocally. Our results suggest that mouse cells lacking functional *Brca1* show a greater propensity for ALT than their *Brca1* proficient counterparts (Fig. 5A). This trend was also evident in the case of human *BRCA1* defective cells albeit but the difference was not statistically significant (Fig. 5B) possibly suggesting a tighter suppression of ALT activity in human cells than in mouse cells.

Previous reports have shown that ALT and telomerase can coexist in the same cells. This is particularly evident in the case of mouse cells. For example, when an external DNA sequence was attached to a single mouse telomere this sequence was copied by other telomeres in somatic cells but not in the germ-line cells (Neumann et al., 2013). This suggests that ALT is heavily suppressed in the mouse germ-line for unknown reasons. Even though human and mouse cells differ significantly in terms of telomere length maintenance, and ALT may be more tightly regulated in human somatic cells (Fig. 5B), telomerase and ALT coexist also in human cells (Henson et al., 2002). Taken together these results point to a scenario in which telomere homeostasis is not a simple game of a single mechanism (telomerase or ALT) but rather a complex interplay of at least two mechanisms (telomerase and ALT), which may operate differently in different species or in different tissues from the same species (Henson et al., 2002).

Interestingly, cells from Friedreich ataxia (FRDA) patients show some evidence for elevated ALT markers. For example, the frequencies of APB-positive foci and T-SCEs are elevated in comparison to control cells (Anjomani Virmouni et al., 2015). Even though this study did not employ the CC assay to assess the ALT activity more conclusively it is extremely rare that primary human cells show elevated APB staining and T-SCE frequencies. FRDA is a neurological disorder characterized by the expansion of GAA repeats within the *FXN* gene (Campuzano et al., 1996). The expansion have been linked with potential defects in mismatch repair (MMR) (Ezzatizadeh et al., 2012). There is some evidence that ALT is activated in gastric cancer cells featuring an MMR defect (Omori et al., 2009) and in the HCT15 colon cancer cell line defective in the MMR protein hMSH6 when telomerase is inhibited (Bechter et al., 2004). Therefore, it is possible that MMR defects alter the balance of telomere homeostasis in favor of ALT.

By the same token, our results argue that defective *BRCA1* alters telomere homeostasis in favor of ALT, perhaps acting as its de-repressor. This finding may have implications for cancer therapy based on targeting telomere maintenance. Attempts to suppress telomerase as part of cancer therapy are likely to lead to a positive selection for cells in which ALT is de-repressed. Thus, the telomerase-based therapy may not work on its own without ensuring that the ALT pathway remains repressed. Further research is needed to identify potential ALT activators and repressors. Our results are consistent with the view that normal BRCA1 acts as a repressor of ALT.

ACKNOWLEDGMENT

We acknowledge Dr Amir Hassan-Khani from Bent-Al-Hoda Hospital Mashhad, Iran, for partly funding Parisa K Kargaran. Supported in part by a grant from the DoReMi consortium, EC.

REFERENCES

Acharya S, Kaul Z, Gocha AS, Martinez AR, Harris J, Parvin JD, Groden J. 2014. Association of BLM and BRCA1 during telomere maintenance in ALT cells. PLoS One 9:e103819.

Al-Wahiby S, Slijepcevic P. 2005. Chromosomal aberrations involving telomeres in BRCA1 deficient human and mouse cell lines. Cytogenet Genome Res 109:491–496.

Anjomani Virmouni S, Al-Mahdawi S, Sandi C, Yasaei H, Giunti P, Slijepcevic P, Pook MA. 2015. Identification of telomere dysfunction in Friedreich ataxia. Mol Neurodegener 10:22. DOI: 10.1186/s13024-015-0019-6.

Badie S, Carlos AR, Folio C, Okamoto K, Bouwman P, Jonkers J, Tarsounas M. 2015. BRCA1 and CtIP promote alternative non-homologous end-joining at uncapped telomeres. EMBO J e201488947.

Bailey SM, Goodwin EH, Cornforth MN. 2004. Strand-specific fluorescence *in situ* hybridization: The CO-FISH family. Cytogenet Genome Res 107:14–17.

Bechter OE, Zou Y, Walker W, Wright WE, Shay JW. 2004. Telomeric recombination in mismatch repair deficient human colon cancer cells after telomerase inhibition. Cancer Res 64:3444–3451.

Blackburn EH, Epel ES, Lin J. 2015. Human telomere biology: A contributory and interactive factor in aging, disease risks, and protection. Science 350:1193–1198.

Blasco MA, Lee HW, Hande MP, Samper E, Lansdorp PM, DePinho RA, Greider CW. 1997. Telomere shortening and tumor formation by mouse cells lacking telomerase RNA. Cell 91:25–34.

Bodvarsdottir SK, Steinarsdottir M, Bjarnason H, Eyfjord JE. 2012. Dysfunctional telomeres in human BRCA2 mutated breast tumors and cell lines. Mutat Res 729:90–99.

Cabuy E, Newton C, Joksic G, Woodbine L, Koller B, Jeggo PA, Slijepcevic P. 2005. Accelerated telomere shortening and telomere abnormalities in radiosensitive cell lines. Radiat Res 164: 53–62.

Cabuy E, Newton C, Roberts T, Newbold R, Slijepcevic P. 2004. Identification of subpopulations of cells with differing telomere lengths in mouse and human cell lines by flow FISH. Cytometry A 62:150–161.

Cabuy E, Newton C, Slijepcevic P. 2008. BRCA1 knock-down causes telomere dysfunction in mammary epithelial cells. Cytogenet Genome Res 122:336–342.

Campuzano V, Montermini L, Molto MD, Pianese L, Cossee M, Cavalcanti F, Monros E, Rodius F, Duclos F, Monticelli A, Zara F, Canizares J, Koutnikova H, Bidichandani SI, Gellera C, Brice A, Trouillas P, De Michele G, Filla A, De Frutos R, Palau F, Patel PI, Di Donato S, Mandel JL, Cocozza S, Koenig M, Pandolfo M. 1996. Friedreich's ataxia: Autosomal recessive disease caused by an intronic GAA triplet repeat expansion. Science 271:1423–1427.

Cao L, Li W, Kim S, Brodie SG, Deng CX. 2003. Senescence, aging, and malignant transformation mediated by p53 in mice lacking the Brca1 full-length isoform. Genes Dev 17:201–213.

Castilla LH, Couch FJ, Erdos MR, Hoskins KF, Calzone K, Garber JE, Boyd J, Lubin MB, Deshano ML, Brody LC, Collins FS, Weber BL. 1994. Mutations in the BRCA1 gene in families with early-onset breast and ovarian cancer. Nat Genet 8:387–391.

Cheng WH, Kusumoto R, Opresko PL, Sui X, Huang S, Nicolette ML, Paull TT, Campisi J, Seidman M, Bohr VA. 2006. Collaboration of Werner syndrome protein and BRCA1 in cellular responses to DNA interstrand cross-links. Nucleic Acids Res 34:2751–2760.

Davalos AR, Campisi J. 2003. Bloom syndrome cells undergo p53-dependent apoptosis and delayed assembly of BRCA1 and NBS1 repair complexes at stalled replication forks. J Cell Biol 162:1197–1209.

de Lange T. 2015. A loopy view of telomere evolution. Front Genet 6. DOI: 10.3389/fgene.2015.00321.

Ezzatizadeh V, Pinto RM, Sandi C, Sandi M, Al-Mahdawi S, te Riele H, Pook MA. 2012. The mismatch repair system protects against intergenerational GAA repeat instability in a Friedreich ataxia mouse model. Neurobiol Dis 46:165–171.

Foray N, Randrianarison V, Marot D, Perricaudet M, Lenoir G, Feunteun J. 1999. Gamma-rays-induced death of human cells carrying mutations of BRCA1 or BRCA2. Oncogene 18:7334–7342.

French JD, Dunn J, Smart CE, Manning N, Brown MA. 2006. Disruption of BRCA1 function results in telomere lengthening and increased anaphase bridge formation in immortalized cell lines. Genes Chromosomes Cancer 45:277–289.

Harley CB, Futcher AB, Greider CW. 1990. Telomeres shorten during ageing of human fibroblasts. Nature 345:458–460.

Henson JD, Cao Y, Huschtscha LI, Chang AC, Au AY, Pickett HA, Reddel RR. 2009. DNA C-circles are specific and quantifiable markers of alternative-lengthening-of-telomeres activity. Nat Biotechnol 27:1181–1185.

Henson JD, Neumann AA, Yeager TR, Reddel RR. 2002. Alternative lengthening of telomeres in mammalian cells. Oncogene 21:598–610.

Henson JD, Reddel RR. 2010. Assaying and investigating alternative lengthening of telomeres activity in human cells and cancers. FEBS Lett 584:3800–3811.

Kim NW, Piatyszek MA, Prowse KR, Harley CB, West MD, Ho PL, Coviello GM, Wright WE, Weinrich SL, Shay JW. 1994. Specific association of human telomerase activity with immortal cells and cancer. Science 266:2011–2015.

Laud PR, Multani AS, Bailey SM, Wu L, Ma J, Kingsley C, Lebel M, Pathak S, DePinho RA, Chang S. 2005. Elevated telomere–telomere recombination in WRN-deficient, telomere dysfunctional cells promotes escape from senescence and engagement of the ALT pathway. Genes Dev 19:2560–2570.

Londono-Vallejo JA, Der-Sarkissian H, Cazes L, Bacchetti S, Reddel RR. 2004. Alternative lengthening of telomeres is characterized by high rates of telomeric exchange. Cancer Res 64: 2324–2327.

Lovejoy CA, Li W, Reisenweber S, Thongthip S, Bruno J, de Lange T, De S, Petrini JH, Sung PA, Jasin M, Rosenbluh J, Zwang Y, Weir BA, Hatton C, Ivanova E, Macconaill L, Hanna M, Hahn WC, Lue NF, Reddel RR, Jiao Y, Kinzler K, Vogelstein B, Papadopoulos N, Meeker AK. 2012. Loss of ATRX, genome instability, and an altered DNA damage response are hallmarks of the alternative lengthening of telomeres pathway. PLoS Genet 8:e1002772.

Maser RS, DePinho RA. 2002. Keeping telomerase in its place. Nat Med 8:934–936.

McIlrath J, Bouffler SD, Samper E, Cuthbert A, Wojcik A, Szumiel I, Bryant PE, Riches AC, Thompson A, Blasco MA, Newbold RF, Slijepcevic P. 2001. Telomere length abnormalities in mammalian radiosensitive cells. Cancer Res 61:912–915.

McPherson JP, Hande MP, Poonepalli A, Lemmers B, Zablocki E, Migon E, Shehabeldin A, Porras A, Karaskova J, Vukovic B, Squire J, Hakem R. 2006. A role for Brca1 in chromosome end maintenance. Hum Mol Genet 15:831–838.

Min J, Choi ES, Hwang K, Kim J, Sampath S, Venkitaraman AR, Lee H. 2012. The breast cancer susceptibility gene BRCA2 is required for the maintenance of telomere homeostasis. J Biol Chem 287:5091–5101.

Moynahan ME, Chiu JW, Koller BH, Jasin M. 1999. Brca1 controls homology-directed DNA repair. Mol Cell 4:511–518.

Neumann AA, Reddel RR. 2006. 7 Telomerase-independent Maintenance of Mammalian Telomeres. Cold Spring Harb Monogr Arch 45:163–198.

Neumann AA, Watson CM, Noble JR, Pickett HA, Tam PP, Reddel RR. 2013. Alternative lengthening of telomeres in normal mammalian somatic cells. Genes Dev 27:18–23.

Ohta T, Sato K, Wu W. 2011. The BRCA1 ubiquitin ligase and homologous recombination repair. FEBS Lett 585:2836–2844.

Ojani M. 2012. PhD Thesis: Relationship between DNA damage response and telomere maintenance: Brunel University London. 200 p.

Omori Y, Nakayama F, Li D, Kanemitsu K, Semba S, Ito A, Yokozaki H. 2009. Alternative lengthening of telomeres frequently occurs in mismatch repair system-deficient gastric carcinoma. Cancer Sci 100:413–418.

Perrem K, Colgin LM, Neumann AA, Yeager TR, Reddel RR. 2001. Coexistence of alternative lengthening of telomeres and telomerase in hTERT-transfected GM847 cells. Mol Cell Biol 21:3862–3875.

Rosen EM. 2013. BRCA1 in the DNA damage response and at telomeres. Front Genet 4:85. DOI: 10.3389/fgene.2013.00085.

Roy R, Chun J, Powell SN. 2012. BRCA1 and BRCA2: Different roles in a common pathway of genome protection. Nat Rev Cancer 12:68–78.

Salk D, Au K, Hoehn H, Martin GM. 1985. Cytogenetic aspects of Werner syndrome. Adv Exp Med Biol 190:541–546.

Sapir E, Gozaly-Chianea Y, Al-Wahiby S, Ravindran S, Yasaei H, Slijepcevic P. 2011. Effects of BRCA2 deficiency on telomere

recombination in non-ALT and ALT cells. Genome Integr 2:9. DOI: 10.1186/2041-9414-2-9.

Sedic M, Skibinski A, Brown N, Gallardo M, Mulligan P, Martinez P, Keller PJ, Glover E, Richardson AL, Cowan J, Toland AE, Ravichandran K, Riethman H, Naber SP, Naar AM, Blasco MA, Hinds PW, Kuperwasser C. 2015. Haploinsufficiency for BRCA1 leads to cell-type-specific genomic instability and premature senescence. Nat Commun 6:7505. DOI: 10.1038/ncomms8505.

Snouwaert JN, Gowen LC, Latour AM, Mohn AR, Xiao A, DiBiase L, Koller BH. 1999. BRCA1 deficient embryonic stem cells display a decreased homologous recombination frequency and an increased frequency of non-homologous recombination that is corrected by expression of a Brca1 transgene. Oncogene 18:7900–7907.

Struewing JP, Brody LC, Erdos MR, Kase RG, Giambarresi TR, Smith SA, Collins FS, Tucker MA. 1995. Detection of eight BRCA1 mutations in 10 breast/ovarian cancer families, including 1 family with male breast cancer. Am J Hum Genet 57:1–7.

Trenz K, Rothfuss A, Schutz P, Speit G. 2002. Mutagen sensitivity of peripheral blood from women carrying a BRCA1 or BRCA2 mutation. Mutat Res 500:89–96.

Turinetto V, Orlando L, Sanchez-Ripoll Y, Kumpfmueller B, Storm MP, Porcedda P, Minieri V, Saviozzi S, Accomasso L, Cibrario Rocchietti E, Moorwood K, Circosta P, Cignetti A, Welham MJ, Giachino C. 2012. High basal gammaH2AX levels sustain self-renewal of mouse embryonic and induced pluripotent stem cells. Stem Cells 30:1414–1423.

Yang G, Rosen DG, Mercado-Uribe I, Colacino JA, Mills GB, Bast RC, Jr., Zhou C, Liu J. 2007. Knockdown of p53 combined with expression of the catalytic subunit of telomerase is sufficient to immortalize primary human ovarian surface epithelial cells. Carcinogenesis 28:174–182.

Yasaei H, Slijepcevic P. 2010. Defective Artemis causes mild telomere dysfunction. Genome Integr 1:3. DOI: 10.1186/2041-9414-1-3.

Yeager TR, Neumann AA, Englezou A, Huschtscha LI, Noble JR, Reddel RR. 1999. Telomerase-negative immortalized human cells contain a novel type of promyelocytic leukemia (PML) body. Cancer Res 59:4175–4179.